EXPERIMENTAL AND NUMERICAL INVESTIGATIONS OF NATURAL CONVECTION IN FREEZING WATER

T.A. Kowalewski, A. Cybulski
Center of Mechanics, IPPT PAN
Polish Academy of Sciences, PL 00-049 Warszawa

ABSTRACT
Thermal convection in a lid cooled cavity with phase change was studied experimentally and numerically. The flow and ice front structures, and their dependence on the flow parameters (Rayleigh number) were investigated. In the experiment, the onset of convection in an initially isothermal fluid (water) in a $38 \times 38 \times 38$mm plexiglas box, which is instantaneously cooled from isothermal top wall to a temperature of -10^oC, has been investigated. The other five walls of the cavity are non-adiabatic, allowing the entry of heat from the external fluid surrounding the cavity. The external temperature was varied from 5^oC to 20^oC. The temperature and velocity fields in the cavity were measured by means of liquid crystals suspended as small tracer particles in the liquid. After the convection starts a complicated flow pattern was observed, which also became visible in the structure of the ice surface. The symmetry of the flow was usually disturbed by existing small imperfection of the cavity and fluctuations of initial field conditions. It was found that the growing ice has a stabilising effect on the flow. The experiments were compared with the 3D numerical simulation using finite-differences code ICE3D.

KEY WORDS: NATURAL CONVECTION, FREEZING, LIQUID CRYSTALS, PIT and PIV

1. INTRODUCTION

The transport of heat or mass by a buoyancy-induced convective motion is a mechanism which is relevant to many physical systems; consequently numerous theoretical, experimental and numerical studies of various aspects of natural convection flows have been performed. When phase change takes place, in our case freezing on the under surface of the lid, both thermal and kinematic boundary conditions of the flow change. It is an additional non-linear coupling complicating the prediction of the flow patterns. Despite the fact that freezing starts at a planar surface, the surface of ice does not remain planar. Its distortion in turn affects the convection in the whole cavity. A complex interaction between the flow, the moving boundary and the latent heat released on the surface decides the flow pattern which is established. Hence, shape and purity of the growing crystal will strongly depend on structure and steadiness of the flow during solidification. The main aim of our investigations to collect more details on the different flow structures and to try to answer the question: Which flow

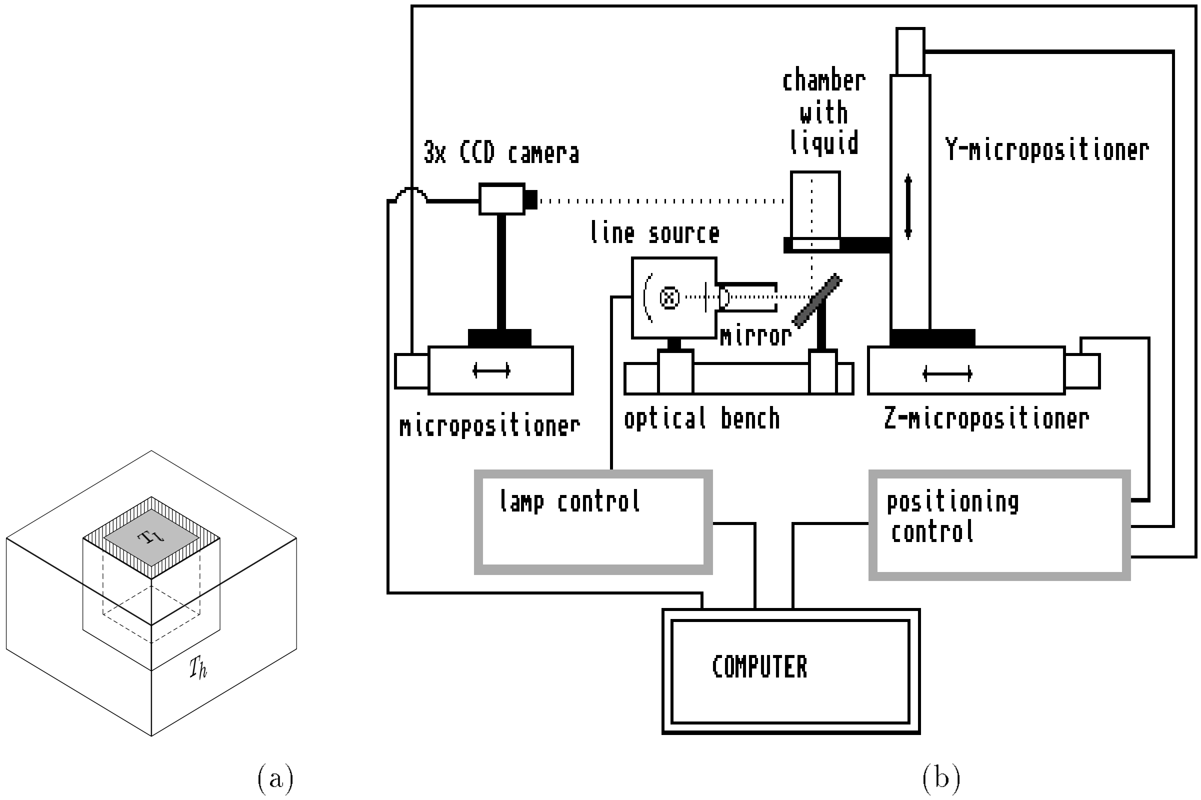

Figure 1: (a) - the cubical box with cooled top surface at T_l, heated by external water bath at temperature T_h; (b) - experimental setup, vertical light sheet configuration.

pattern will be selected for given real flow conditions, and is it possible to control such a selection with the help of imposed initial flow conditions and imposed boundary conditions?

2. FORMULATION OF THE PROBLEM

We consider the convective flow in a cubical box filled with a viscous heat conducting liquid. The fluid density, viscosity, thermal conductivity and heat capacity are assumed to be temperature dependent. The flow takes place in a container with an aspect ratio of one. The top surface of the cavity is isothermal at temperature $T_l = -10^oC$. The thermal boundary condition for the top surface of the fluid domain (the ice-water interface) is assumed isothermal at the temperature $T_c = 0^oC$. The other five walls are non-adiabatic, allowing the entry of heat from the external fluid which surrounds the cavity (Fig. 1a). The temperature of the fluid in the external bath $T_h > T_c$ is constant. Due to forced convection in the bath the temperature at the external surfaces of the box is close to T_h. The temperature field at the inner surfaces of the walls adjusts itself depending on both the flow inside the box and the heat flux through and along the walls. The initial fluid temperature and temperature of all six walls is T_h. Convection starts when, at time $t = 0$, the lid temperature drops to T_l.

The three basic dimensionless parameters defining the problem, the Rayleigh number (Ra) the Prandtl number (Pr) and the Stefan number (Ste)

$$Ra = \frac{g\beta\Delta T H^3}{\kappa\nu}\ , \qquad Pr = \frac{\nu}{\kappa}\ , \qquad Ste = \frac{c_p\Delta T}{L_f}, \tag{1}$$

are used to characterise and compare the numerical and experimental results.

In the above definitions, g, H, ΔT, κ, β, ν, c_p, L_f denote respectively the gravitational acceleration, the cavity height, the temperature difference $T_h - T_c$, the thermal diffusivity, the coefficient of thermal expansion, the kinematic viscosity, the specific heat and the latent heat of fusion. The non-dimensional temperature is defined as: $\theta = (T - T_c)/\Delta T$.

2.1 Numerical model

A numerical simulation of the problem was performed using a finite difference model of the Navier-Stokes and energy equations. A three-dimensional numerical code ICE3D (Yeoh [1993]) have been used. The code allows to study transient convection with phase change in a fluid with temperature-dependent properties. The vorticity-vector potential formulation (Mallinson & de Vahl Davis [1977]) is used in the code. When phase change takes place, the movement of the solid-liquid interface is computed with the use of an energy balance at the interface which incorporates the latent energy transfer accompanying phase change. As the physical domain changes in shape, the interface boundary grid must be generated at each time step, following which a new computational grid is determined in the liquid and solid regions. Independent conservation equations are solved for each phase and are coupled by the condition at the solid-liquid interface. Transformation techniques were used to map the moving physical domain onto the computational domain.

When simulating experimental conditions, the main problem which arises is the proper definition of thermal boundary conditions (TBC). The definition of TBC in the code is sufficiently flexible to allow the imposition of an arbitrary temperature, a specified heat flux or a specified heat transfer coefficient on each of the six surfaces of the box.

Solutions were obtained using a $45 \times 45 \times 45$ mesh for the fluid domain and $45 \times 45 \times 7$ mesh points for the solid domain (ice). To start the calculations, it is assumed that at the first instance the lid is already covered with $0.02 \times H$ layer of the ice.

3. EXPERIMENTAL

The experimental set-up used to acquire temperature and velocity fields consists of the convection box, a halogen tube lamp and a CCD colour camera. The box, of 38mm inner dimension, has an isothermal lid made of a black anodised metal and five 8 mm thick plexiglas walls (Fig. 1a). The lid was maintained at a constant temperature by anti-freeze coolant flowing through internal channels in the metal plate. The temperature of the liquid cooling the lid and of that of water in the bath surrounding the five non-adiabatic walls was controlled by thermostats. Initially the cavity and the lid were at the same temperature T_h. The cooling of the lid was started abruptly by opening the inlet valves to the coolant passages. The temperature at the lid and at a few control points inside the cavity was continuously monitored using thermocouples. Distilled water was used in the experiments.

Four experiments were performed with phase change when the lid was suddenly cooled (in practice, within a time of about 90 seconds) from the initial fluid and surrounding water bath temperature T_h to a temperature of T_l. In the experiments $T_l = -10°C$ and T_h was set to 5, 10, 15, or $20°C$, respectively. The formation of ice on the lid established the solid-liquid interface temperature at $0°C$. Hence, the temperature difference ΔT in the water varied in the experiments from 5 to $20K$. The corresponding values of Rayleigh number for the four experiments was respectively $Ra = 7.77 \times 10^5$, $Ra = 1.56 \times 10^6$, $Ra = 2.33 \times 10^6$, and $Ra = 3.11 \times 10^6$, and of the Stefan number $Ste = 0.063$, 0.125, 0.189 and 0.252. The Prandtl number was $Pr = 13.3$.

The flow was observed at various vertical and horizontal cross sections of the cavity using a light sheet technique. The halogen tube generated a 2 mm thick sheet of white light, which illuminated the selected cross-section of the flow. The system of three step-motors combined with mirror allowed to acquire images of the several cross-section fully automatically within few seconds (Fig. 1b). Hence, due to relatively slow variations of the flow structures our system allows transient recording of main three-dimensional flow features.

The temperature and velocity fields were simultaneously measured by means of thermochromic liquid crystals (TLC) suspended as small (about $50\mu m$) tracer particles in the liquid (Hiller et al. [1993]). The Particle Image Thermometry (PIT) is based on temperature-dependent reflectivity of TLC at the visible light wavelengths. If TLC are illuminated with white light, then the colour of the light they reflect changes from red to blue when the temperature is raised. This occurs within a well defined temperature range (the so called colour play range), which depends on the type of TLC used. A three chip CCD colour camera (JVC KYF55), which gives an RGB-signal for the red, green and blue portions of the incoming light, was used to observe the flow. At each time step four images of $768(H) \times 512(V)$ pixels density were acquired by 8-bit digitising board VFG100 (Imaging Technology Inc.) To get colour information of TLC tracers the first three images from red, green and blue channel of the camera were used. The colour play of TLC was specially adopted to cover interesting us temperature range from 0^oC to about 6^oC. To evaluate the temperature the modified HSI representation of the RGB space was used. The 8-bit RGB information was transformed pixel by pixel into intensity (I), saturation (S) and hue (H) according to the following relations:

$$I = \sqrt{(R^2 + G^2 + B^2)}/\sqrt{3}\,, \qquad S = 255 \cdot (1 - min(R, G, B)/I) \tag{2}$$

$$H = \begin{cases} 63 + ((G' - R') \cdot 63)/(G' + R') & \text{if } B' = 0 \\ 189 + ((B' - G') \cdot 63)/(B' + G') & \text{if } R' = 0 \end{cases} \tag{3}$$

where R', G', B' are obtained by subtracting from R, G, and B their common minimum. This corresponds to subtracting non-interesting us white light part of the signal. By 8-bit discretisation of the RGB signals the value of hue varies on the chromaticity diagram over the range 0–252. As liquid crystals reflect pure spectral colours, there are no hue values recorded simultaneously by the blue- and red- sensitive chips of the camera. Therefore, the shrunken hue representation is fully justified, improving the colour (i.e. temperature) resolution of the method. Temperature is determined by relating the hue to a temperature calibration function. The calibration is performed at the experimental conditions, by gradually increasing the temperature in the entire uniformly heated cavity (in steps of 0.1 - 0.5 K), and evaluating the hue of light reflected from tracers. The non-linear relation between temperature and hue is described by a 8th order polynomial fitted to the points (Fig. 2) measured for TLC used. The recorded information were processed using median and averaging filters. The contouring algorithms were applied to reproduce results in the form of a temperature map (isotherms). The accuracy of the measured temperature depends on the hue value, and varies from $\pm 2.5\%$ at the low end to $\pm 10\%$ at the high end of the covered temperature range.

The velocity fields were measured by Particle Image Velocimetry (PIV) using two separately captured digital images taken at a constant time interval (typically 5s). Each of the images taken shows

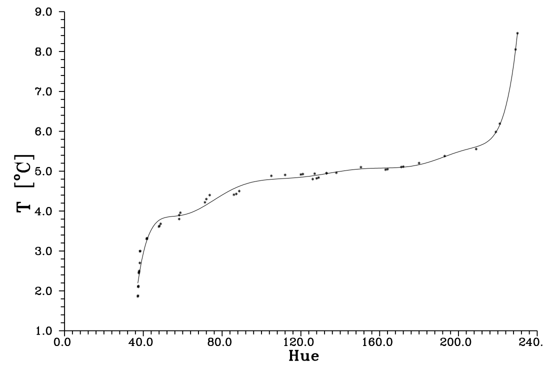

Figure 2: Temperature calibration curve of temperature as a function of the hue values evaluated from the light reflected by TLC mixture used. The hue varies from red (0), through green (126) to blue (252).

a relatively dense cloud of single illuminated particles (TLC). The PIV evaluation was performed by cross-correlating an image from the blue channel of the colour triple with additional fourth image taken from the blue channel only. The magnitude and direction of the velocity vectors were obtained applying FFT to evaluate a cross-correlation function subsequent for small sections of the whole image. Typically image of 480x480 pixels was divided into 32x32 pixel matrices, which were spaced every 16 pixels (partly overlapping each other). To improve accuracy of the evaluation procedure, special filtering techniques based on local contrasting the images were developed. The evaluation of images was mainly performed on an Pentium (133MHz) personal computer under Linux OS. The analysis of one pair of images took about 2 minutes.

To obtain a general view of the flow pattern, several images were recorded periodically within a given time interval and were then superimposed in the computer. Displayed images are similar to multiple exposure photographs, showing the flow direction and its structure.

The recording of the flow fields was performed periodically (every 30-60s), beginning 1 minute after the start of cooling. The recorded digitised images were stored on the hard disk of the computer (PC 386) for later evaluation. Typically one experiment consisted of 200×4 8-bit images, exceeding 300MB storage place. Besides the further image processing, the computer also controlled the experimental conditions, i.e. the illumination, the wall temperatures, the recording sequences, and the positions of the cavity and camera.

4. RESULTS

Two particular aspects of the flow were investigated in the experiments: (i) the formation of the ice crystal and (ii) the development of the ice front and its interaction with the convective flow structure.

In the preliminary experiments it was observed that often growing ice appeared optically unclean. The ice varied from clear crystal to "milky" structure filled with "dendrite like" inclusions. Hence, in the separate experiments several combination of freezing parameters were tested in the cavity filled with distilled, degasified water. These investigations can be summarised in the following way:

i. Between two vertical configurations of solidification, namely freezing from the lid and from the bottom, the first one gives more homogeneous and clear ice structure.

ii. Increasing temperature gradient usually improves quality of the ice crystal.

iii. The subcooling necessary to initiate ice growth is about -7^oC in the experiments performed.

iv. The "dendrites" observed in larger or smaller amount for all investigated cases form relatively regular "hedgehog" like structure (Fig. 3). They appeared already in the initial state of freezing. Careful observations allowed to identify them as a long, about $200\mu m$ in diameter tubes, filled with

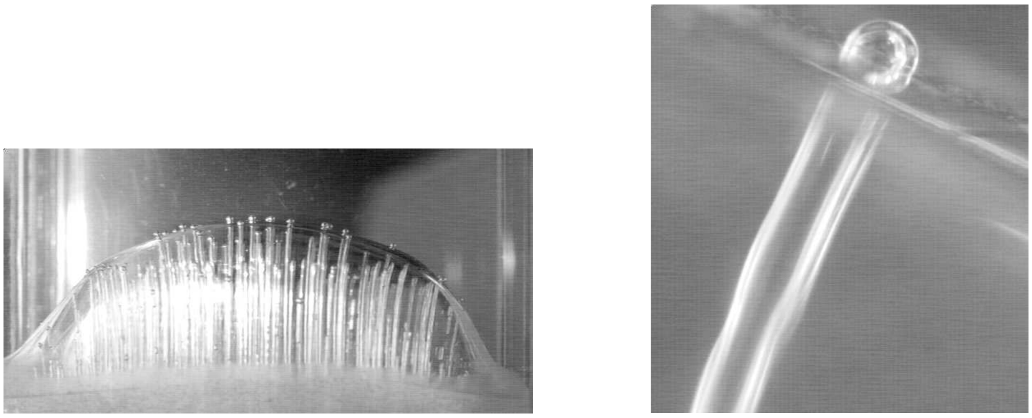

Figure 3: Freezing of water from the cooled bottom. Growing inclusions and close-up of their single structure.

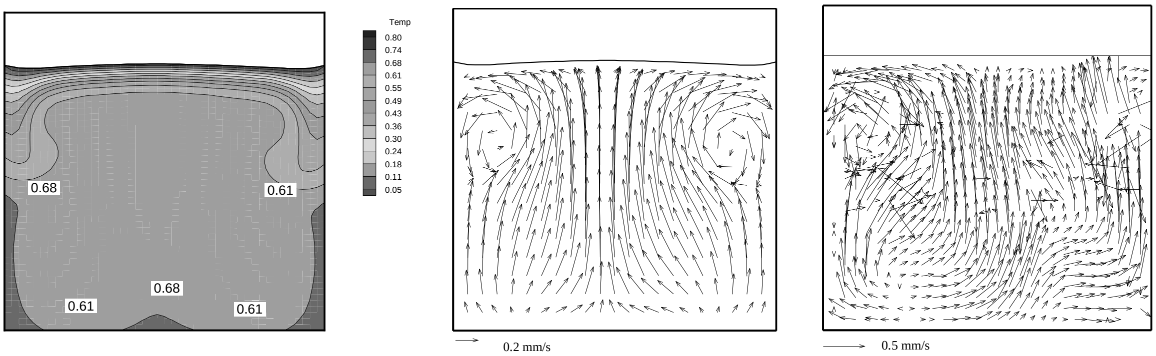

(a) (b) (c)

Figure 4: Onset of convection for $\Delta T = 100^oC$ ($Ra = 1.56 \cdot 10^6$) in centre vertical plane at time step 600s. Numerical results for (a) - non-dimensional temperature, and (b) - velocity; (c) - measured (PIV) velocity field.

air trapped in ice. It is seems that in water, even after intensive degasification under vacuum, enough air may be released during the fusion process to form observed "tubes".

Besides of our general interest to form a pure ice crystals, the presence of inclusion in the solid may apparently modify its thermal properties. This fact has to be taken into account, when comparing numerical and experimental results.

In the following experiments the ice formation was studied by decreasing the lid temperature to -10^oC. When the top wall was suddenly cooled a cold thermal boundary layer appeared. The presence of temperature gradient in the liquid will, in most cases, activate natural convection. Under these conditions, the heat conduction problem in the solid is modified by convective heat transfer from the liquid. However, the presence of temperature variations in the liquid does not lead immediately to natural convection motions. A stable stratification was observed for a thin (0.5mm) layer of the subcooled water adjacent to the lid. The water density anomaly probably additionally stabilise such configuration. The natural convection occurred then, when an instability threshold was achieved. Before first solidification layer appeared, several small mushroom like "termics" dropped down from the thermal layer. Generally, for all observed cases flow structure was initially unstable and asymmetric, and only after long enough time eventually symmetric flow appeared. The flow

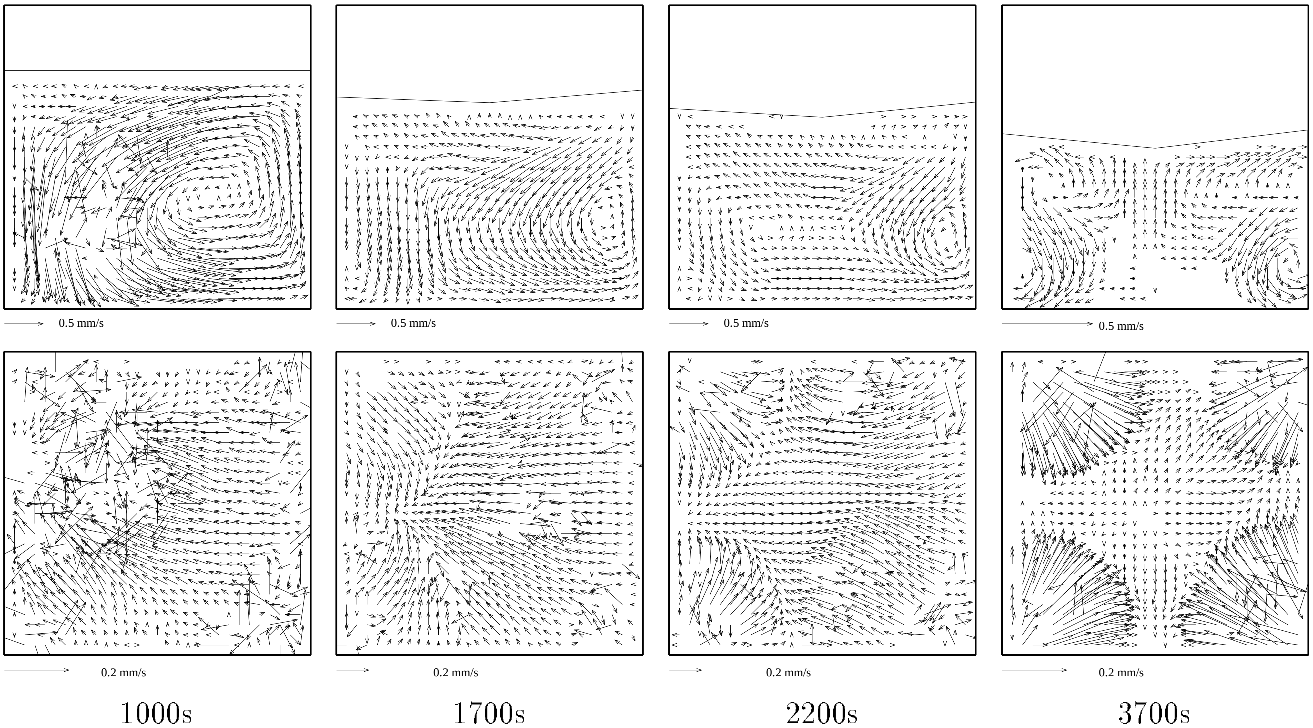

Figure 5: Measured velocity fields (PIV) at four time steps; (top row) - centre vertical cross-section, (bottom row) - centre horizontal cross-sections.

pattern stabilised faster for higher external temperature and also when the ice front was already well developed.

For small external temperature ($T_h = 5^oC$ and 10^oC) the ice front propagates from the lid quite uniformly. Due to the water density anomaly convection has small amplitude for these cases. Especially for $T_h = 5^oC$ only slight modification of the uniform vertical temperature stratification was observed. The ice surface was flat except small wall regions. Initially the observed flow structure was usually asymmetric and very sensitive to external disturbances. A typical transient development of the flow field is shown in Figs.4, 5 for vertical and horizontal centre cross-sections. The strongly asymmetric convective flow (Fig. 4c) initiated also some deformation of the ice front. Such asymmetry, however less visible, is present also in the numerical simulation (Fig. 4a,b). However, in long term the flow pattern and the ice front "selected" their nearly symmetric form. It was characteristic for all four investigated cases, however the time scale for reaching symmetry varied. The nearly symmetric equilibrium state seemed to be the stead state. It was reached asymptotically after long time of several hours. A complicated flow pattern appeared after convection started at the higher Rayleigh numbers (external temperatures $T_h = 15^oC$ and 20^oC). Within the first 30s-50s the first thin layer of ice appeared. But observed flow was unstable, breaking down into few plumes falling down along the side walls. This flow, in turn, generated several recalculating zones, transporting heat and vorticity from the side walls to the centre. It took 10 to 20 minutes after a general flow pattern was established, with a downward flowing central "jet" of cold liquid and reversal flow along the side walls. From this time also recirculation zone, due to water density anomaly could be identified close to the ice surface (Fig. 6a,b). There is a primary cell which carries hot fluid up the wall to the ice interface, resulting in a cutting back of the outer edges of this interface; water then flows down

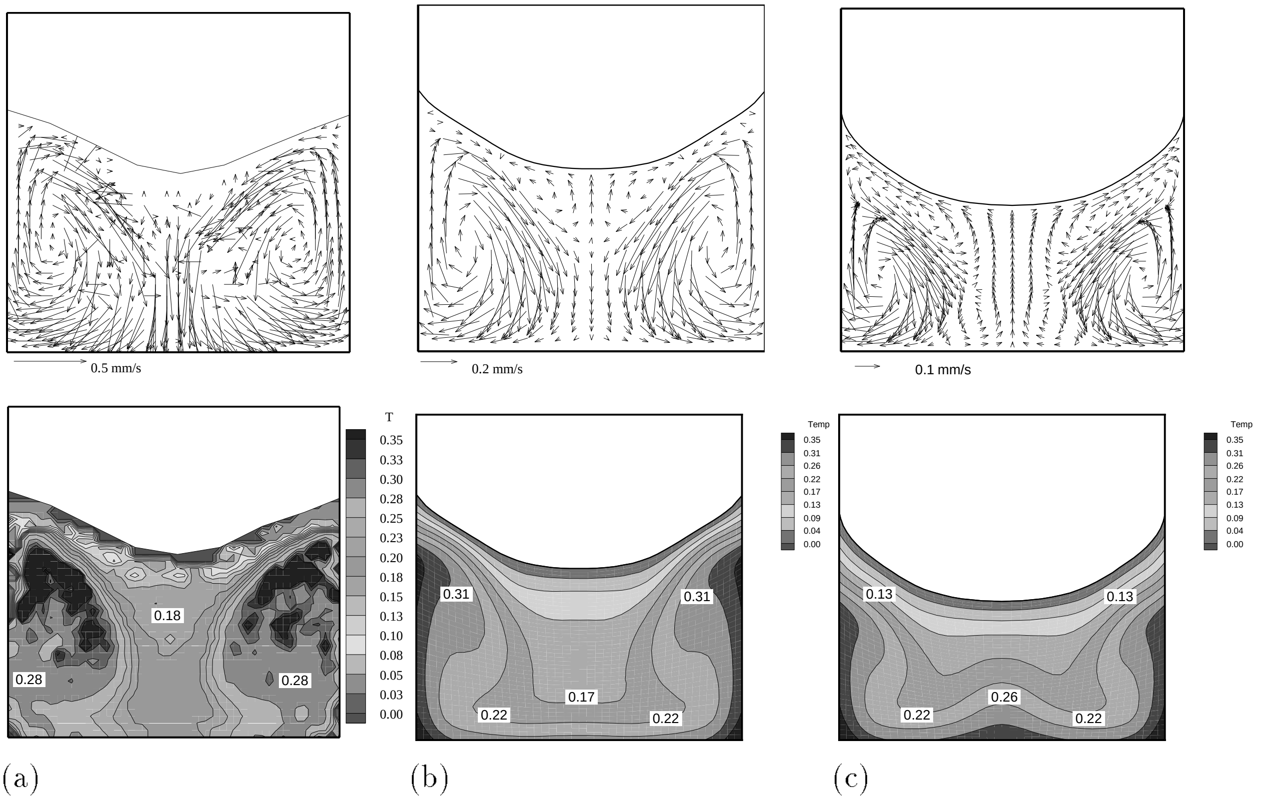

Figure 6: Velocity (top row) and non-dimensional temperature (bottom row) fields for $\Delta T = 20^o C$. (a)- measured at $t = 20400s$, (b) - numerical at $t = 3700s$, (c) - numerical steady state.

in the centre of the cavity. Just below the ice in the centre of the cavity there were small counter rotating secondary flows established due to the density extreme of water in this region. At some distance from the ice surface this flow obviously "collide" with the hot liquid rising from the bottom and along the side wall. This could be clearly seen in the particle tracks. The flow pattern was manifested in the complex structure of the ice surface (Fig.7a). Recirculating flow and hot reversal circulation along the side walls created a "diamond–like" pattern of the ice front. It was found that for the higher Rayleigh numbers of experiments 3 and 4 the creation of the strongly deformed ice front had a stabilising effect on the flow. The diamond shaped pattern of the ice–fluid interface imposes the direction and character of the flow, faster eliminating the instabilities observed for the previously mentioned freezing from the flat interface. However, due to the initial perturbations, the flow symmetry was not preserved in the experiments and only eventually recovered in the final state (after several hours).

The over-sensitivity of the initial flow pattern was observed also in the numerical simulation. Addition of small perturbation (0.1%) to the initial temperature field resulted in strong asymmetrical flow before apparently "final" configuration with a single cold downward flowing jet along the cavity axis was established (Fig. 6b). Due to long computational time it was impossibly to find the final state by transient calculations. Hence, the steady state was found using "false transient" method (Fig. 6c). It can be seen that between time step $3700s$ and the final state distinct changes of the flow pattern took place. The inverse recirculation zone enlarged. The "central jet" reversed direction and additional two small recirculation "bubbles" appeared in the centre bottom region. These seems to isolate the ice surface from the "hot" jet flowing along side walls, helping to establish the steady

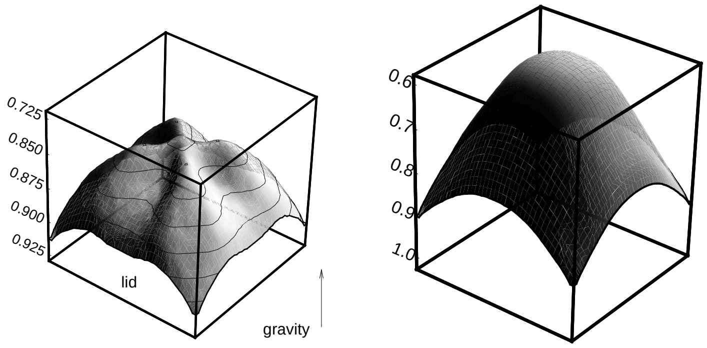

Figure 7: Ice formation under the lid. Ice surface calculated at 6 min (a) and 60 min (b) after the cooling started. The interface is seen from below. $Ra = 3.11 \times 10^6$.

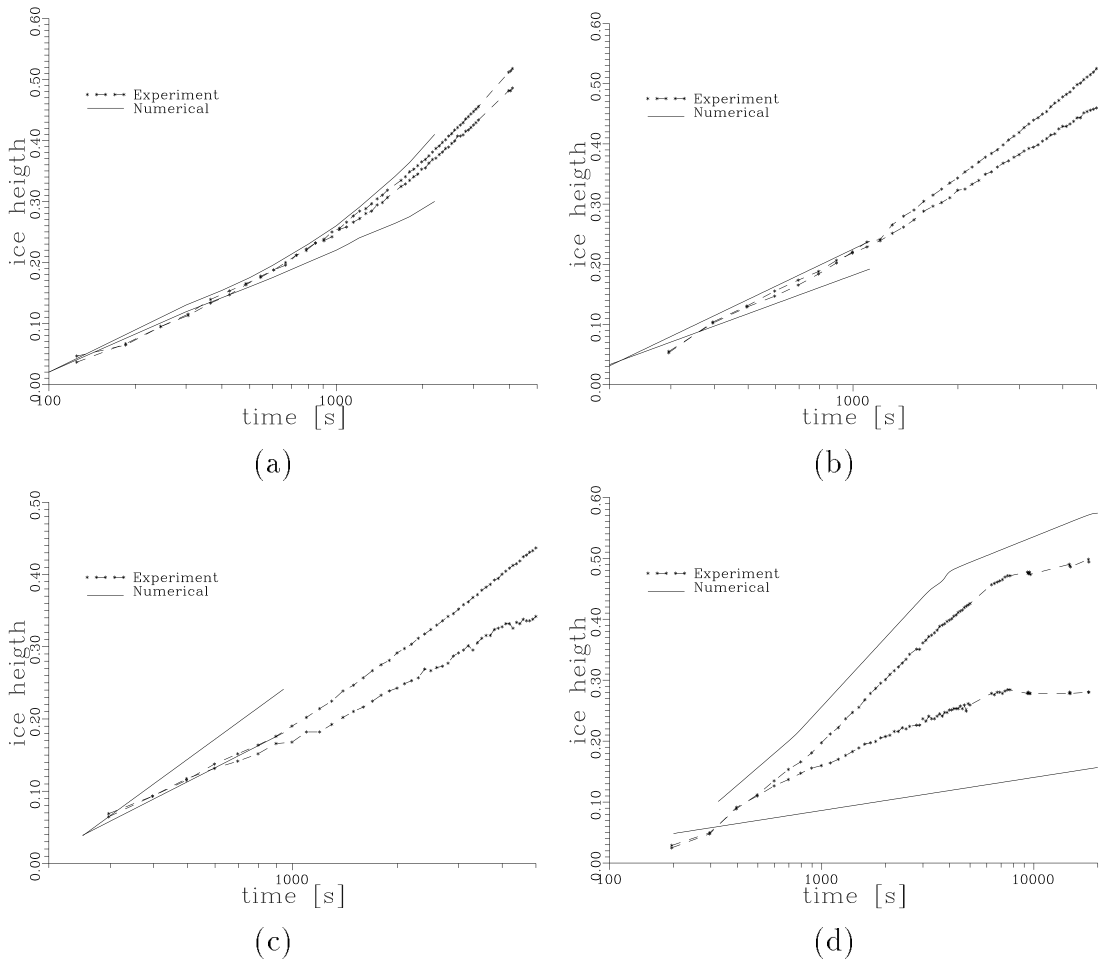

Figure 8: Measured (symbols) and calculated (solid line) ice interface growth rate; maximum and minimum surface height. $T_h =$ (a) 5^oC, (b) 10^oC, (c) 15^oC, (d) 20^oC

state. Using "false transient" method it was impossible to find time necessary to reach the steady state. Obviously, after 6 hours time lap the experimental data (Fig. 6a) are still closer to their "1 hour" numerical counterpart (Fig. 6b).

Figure 8 shows the variation in time of the height of the ice front at the centre of the cavity for the four investigated cases. For the lower Rayleigh number range ($\Delta T = 5 - 10^oC$) there is relatively good agreement between experiment and computations, although as can be seen the numerical model predicted a higher rate of ice growth and higher curvature of the surface. The differences increase with time and for higher Rayleigh numbers became quite serious. This can be consistent with our former hypothesis that the heat transfer rate in the experiments was higher than estimated and used in the model. Neglected heat conduction along the side walls seems to be the main reason (Abegg et al. [1994], Söller et al. [1995]).

5. CONCLUDING REMARKS

The simultaneous measurement of flow and temperature fields using liquid crystals as tracers allowed a qualitative description to be made of the onset of convection generated combined with freezing. However, the instability of the initial state and observed asymmetry of the flow did not permitted direct comparison of the flow fields with their numerical counterparts. The general characteristics like growth rate were well reproduced only for the initial state. The experimental results close to the "symmetrical" case (above 1 hour state) showed qualitative agreement in the velocity and temperature fields with their numerical counterparts. The differences found in the details of the flow pattern and temperature fields are believed to result from differences in the previous flow history (e.g. degree of asymmetry), inappropriately specified TBC on the non-adiabatic walls and also numerical difficulties of modelling regions of colliding boundary layers.

Acknowledgements - The authors are indebted to G. de Vahl Davis, E. Leonardi (UNSW) and G. Yeoh for their computer code ICE3D. This work was supported by the Polish Scientific Committee (KBN Grant No. 3P40400107). The numerical computations were partly performed on CRAY-CS6400 at the Technical University Warsaw (COI).

REFERENCES

Yeoh, G.H. 1993. Natural convection in a solidifying liquid, Ph.D. thesis, University of New South Wales, Kensington, Australia.

Mallinson, G.D. & de Vahl Davis, G. 1977. Three-dimensional natural convection in a box: a numerical study, *J. Fluid Mech.*, **83**, pp. 1-31.

Hiller, W.J., Koch, St., Kowalewski, T.A. & Stella, F. 1993. Onset of natural convection in a cube, *Int. J. Heat Mass Transfer*, **36**, pp. 3251-3263.

Abegg C., de Vahl Davis G., Hiller W.J., Koch St., Kowalewski T.A., Leonardi E., Yeoh G.H., 1994. Experimental and numerical study of three-dimensional natural convection and freezing in water, *Heat Transfer 1994*, **4**, Edt. G.F. Hewitt, IChemE Rugby, pp.1-6.

Söller C., Hiller W.J., Kowalewski T.A. & Leonardi E. 1995. Experimental and numerical investigation of convection in lid cooled cavities — effects of non-ideal thermal boundary conditions on three-dimensional flow, The 3rd ICIAM Congress, July 1995, Hamburg.